

# Investigating the mechanical properties of Al7075 metal matrix composite with improved performance through the incorporation of Fe<sub>3</sub>O<sub>4</sub> and RHS.

Angadi Seshappa<sup>1\*</sup>, Pidaparthy Maheshbabu<sup>2</sup>, Bhavanasi Subbaratnam<sup>3</sup>, Sarella Naresh Kumar<sup>4</sup>, Jajimoggala Sravanthi<sup>5</sup>, Navdeep Singh<sup>6</sup>

<sup>1</sup>Department of Mechanical Engineering, KG Reddy College of Engineering and Technology, Hyderabad, 501501, India.

<sup>2</sup>Department of Mechanical Engineering, CMR College of Engineering & Technology (Autonomous), Hyderabad. Hyderabad-501xxx, India.

<sup>3</sup>Department of Mechanical Engineering, Malla Reddy Engineering College and Management Sciences, Hyderabad-501401, India.

<sup>4</sup>Department of Mechanical Engineering, Vardhaman College of Engineering, and Technology Hyderabad-501218, India

<sup>5</sup>Department of CSE, GRIET, Hyderabad, Telangana, India

<sup>6</sup>Lovely Professional University, Phagwara, Punjab, India.

**Abstract.** Heavily employed in engineering, Metal Matrix Composites are the primary focus of this research. Metal Matrix Composites have much improved mechanical properties and find extensive use across several sectors, including automotive and aerospace. The experiment entails using aluminium (Al7075) as the base material and incorporating iron oxide and RHS in weight ratios of 3%, 6%, and 9% to fabricate a strengthened Metal Matrix Composite. The stir-casting technique is used for the fabrication of these composites. The stir casting technology is selected because to its advantages, including its straightforward manufacturing process, cost efficiency, and reliable distribution of reinforced particles. The Fe<sub>3</sub>O<sub>4</sub> reinforcing particle and RHS have a significant impact on the engineering material properties. The examination revealed enhancements in mechanical properties, including tensile, compression, and hardness strengths. The tensile strength of the 9% wt. reinforced Fe<sub>3</sub>O<sub>4</sub> and RHS is found to be the highest at 362 MPa, while the yield strength is measured at 262 MPa, when compared to the original Al-7075 alloy. Furthermore, the recently manufactured Al7075/Fe<sub>3</sub>O<sub>4</sub> and RHS Metal Matrix Composite were subjected to microstructural examinations using SEM and EDS methodologies. The investigations demonstrated a uniform and homogeneous dispersion of Fe<sub>3</sub>O<sub>4</sub> and RHS reinforced particles inside the composite material.

---

\* Corresponding author: [a.seshappa@kgr.ac.in](mailto:a.seshappa@kgr.ac.in)

## 1 Introduction

In the category of super-high strength deformation alloys, Al-7075 is a precipitation-hardened alloy that has amazing strength, specific stiffness, excellent fracture toughness, corrosion resistance, and great moulding performance and performance. Due to the fact that it is an aluminium alloy, it has distinctive characteristics, which makes it a flexible option for a variety of applications [1–4]. Metals combination particulates. solidifying particulates, acquire construction, along with displacement represent just a few of the unusual qualities that make it among among the most important materials for structure in the aerospace and automotive industries [5–6]. It is better advantageous to use great aqueous analysing approach as opposed with the effective analysing methodology since unique aqueous analysing methodology is higher cost-effective that has enough ability to manufacture complicated morphological elements. Despite this, one of the most significant difficulties associated with its aqueous approach is the achievement of a proportionate the allocation of reinforcements as well as its development of a strong interfacial interaction between the reinforcement and the matrix[7]. An increase in the Al/Fe<sub>3</sub>O<sub>4</sub> Metal Matrix composite results in an increase in both the hardness and tensile strength of the material, but at the expense of ductility in comparison to the base alloy. Additionally, the material exhibits a ductile mode of failure [8].

In the field of mechanical characterization of Fe<sub>3</sub>O<sub>4</sub> and RHS reinforced with Al-7075 matrix composite, there has been a limited amount of work and research described. The stir casting process uses an electric melting furnace to create the suggested Metal Matrix Composite for the purpose of the current experimental investigation.

The aim of the proposed work is to fabricated an Al-7075 Metal Matrix Composite reinforced with Fe<sub>3</sub>O<sub>4</sub>/RHS(weight proportions) in order to determine the optimized weight quantity of Fe<sub>3</sub>O<sub>4</sub>/RHS. The composite's Tensile, compression, Hardness strengths and micro structural characteristic were tabulated and shown.

## 2 Materials and Methods

The Al7075 alloy was used as a base metal in the research project for the purpose of fabricating a composite material that was reinforced with varying weight fractions of Fe Fe<sub>3</sub>O<sub>4</sub>/RHS (three percent, six percent, and nine percent by weight).

Table1 provides an overview of the chemical components that make up aluminium. We decided to use Fe<sub>3</sub>O<sub>4</sub>/RHS 300Mesh particle sizes.

The construction of the aluminium metal matrix composite was accomplished via the use of the stir casting technique. A depiction of the casting setup and the stirrer that is attached to the variable speed motor can be seen in Figure 1. Figure 2 is a flowchart that demonstrates the manufacturing process.

**Table 1:** Chemical Compositions of Aluminum7075.

Constituent	Cu	Cr	Ti	Mg	Zn	Fe	Mn	Si	Al
Percentage in Wt.	1.8	0.2	0.15	1.9	3.25	0.5	0.4	0.5	Balance



**Fig. 1.** Squeeze casting setup for MMC processing

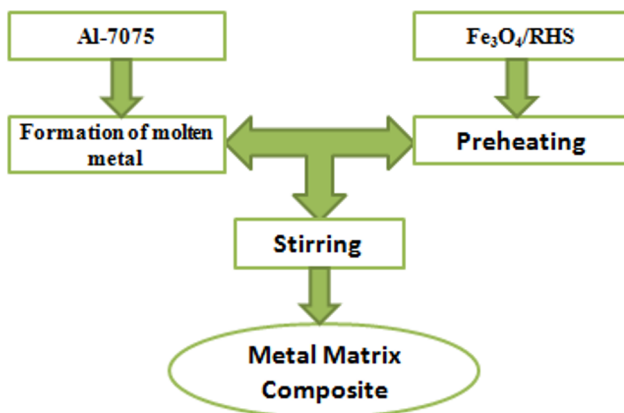


**Fig. 2.** Flow chart for proposed fabricated process.

- ✓ In order to achieve the desired temperature of 660 degrees Celsius, the crucible containing the weighed aluminium alloy 7075 was heated. The crucible was held in the furnace at the same temperature.
- ✓ Based on the weighted proportion of iron oxide and RHS particles, which were 3%, 6%, and 9% respectively.
- ✓ In addition, the moulding dies were heated beforehand.
- ✓ To prevent blowholes and to decrease porosity, it is necessary to include degasifying chemicals.
- ✓ When the temperature reaches the necessary amount, add the determined proportion of iron oxide ( $\text{Fe}_3\text{O}_4$ ) and RHS to the molten metal and mix it well at a speed of 400 revolutions per minute throughout the process.
- ✓ Take out the slag.
- ✓ Let the molten metal pour into the die, and then wait for it to cool down.

Using a universal testing equipment manufactured by Instron and a displacement control mode rate of 0.1 mm/min for testing, tensile and compression work pieces are machined

from rough castings with dimensions of 9 millimetres in diameter and 45 millimetres in gauge length in accordance with ASTM requirements. Several other kinds of testing were carried out, and the greatest results were averaged. We examined a number of different tensile characteristics and percentage elongation for Al-7075 alloy, Al-7075- 3, 6, and 9 weight percent  $\text{Fe}_3\text{O}_4$ /RHS composites. In addition, a compression test was carried out on the same machine in accordance with the criteria of ASTM. Scanning electron microscopy was used in order to do the micro structural examination on the composites that had earlier been created. After being cut from the castings and given a thorough polish, the test sample has a diameter of between 10 and 12 millimetres.

### 3 Findings and Analysis

#### 3.1. Maximum pull-out force when conduct a tensile test

Figure 3 illustrates the ultimate tensile strength (UTS) of the material in comparison to various percentages of  $\text{Fe}_3\text{O}_4$ /RHS. In the presence of a 0–9% weight addition of  $\text{Fe}_3\text{O}_4$ /RHS, there is a discernible increase in UTS, which may range from 190 MPa to 348 MPa across the board.

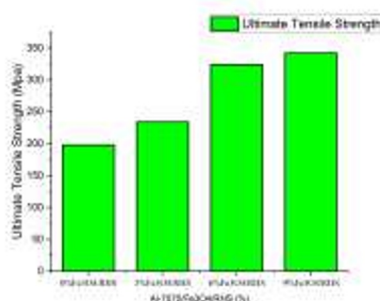


**Fig.3.** Composite Al7075 + Fe3O4/PKSA 0–9% composite ultimate tensile strength.

This consistent rise highlights the significant role that  $\text{Fe}_3\text{O}_4$ /RHS particulates play in determining the mechanical characteristics of the composite, notably in terms of increasing the tensile strength of the material of the composite. Incorporating different amounts of  $\text{Fe}_3\text{O}_4$ /RHS into the material has a favourable influence on the overall mechanical performance of the material, as shown by the observed intensification in tensile strength.

#### 3.2. Strength for yielding

Figure 4 illustrates the composition of the ratio of yield strength to weight %. As the weight percentage of  $\text{Fe}_3\text{O}_4$ /RHS grows from 0% to 9%, the graph clearly demonstrates a significant improvement in yield strength, which goes from 103.6 MPa to 262.16 MPa. This improvement is a clear indication of the increase in yield strength. This trend highlights the good impact that  $\text{Fe}_3\text{O}_4$ /RHS has, demonstrating a considerable increase in the material's yield strength. Therefore, it is important to note that this trend. The fact that the yield strength of the Al7075 metal matrix composite increased as a result of the gradual addition of  $\text{Fe}_3\text{O}_4$ /RHS demonstrates that this reinforcement is effective in improving the overall mechanical characteristics of the composite material.

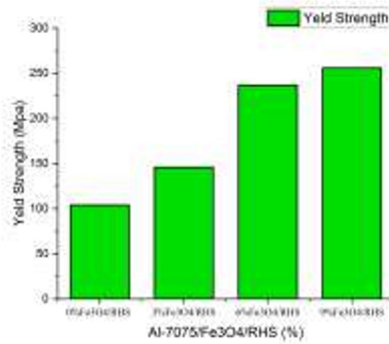


**Fig. 4.** Composite strength - Al-7075/Fe<sub>3</sub>O<sub>4</sub>/PKSA 0 to 9 weight percent.

In addition to contributing to the composite's better mechanical characteristics, the tight arrangement of Fe<sub>3</sub>O<sub>4</sub>/RHS particles is responsible for the increased yield strength. This arrangement also helps to reinforce the molecular strength inside the aluminium lattice for the composite.

### 3.3. Measurement of the percentage of elongation

Figure 5 is a graph that illustrates the effect that Fe<sub>3</sub>O<sub>4</sub>/RHS has on the malleability of the composite material. The graph shows a downward trend when Fe<sub>3</sub>O<sub>4</sub>/RHS particles are added, with the percentages ranging from 0 to 9 weight percent. The integration of Fe<sub>3</sub>O<sub>4</sub>/RHS into the composite product resulted in an increase in the composite's strength, which is the cause of this reduction. The reduction in malleability that was found highlights the trade-off that exists between strength and malleability, indicating the significant influence that different percentages of Fe<sub>3</sub>O<sub>4</sub>/RHS have on the mechanical behaviour of the material.

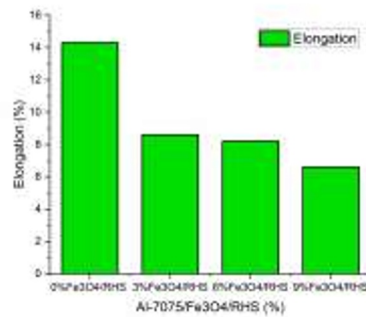


**Fig. 5.** Elongation proportion of Al7075/Fe<sub>3</sub>O<sub>4</sub>/PKSA 0–9 weight percent composite.

### 3.4. Examination of compression

A representation of the compression strength of Al-7075 in the presence of Fe<sub>3</sub>O<sub>4</sub>/RHS composites ranging from 0 to 9 weight percent is shown in Figure 6. Beginning at 629.5 MPa and continuing all the way up to 787.52 MPa, the compression strength shows a progressive rise. This increased trend demonstrates the good influence that the gradual addition of Fe<sub>3</sub>O<sub>4</sub>/RHS has had, confirming the function that it plays in increasing the

compression strength of the composite. Elucidating the possibilities for customising the material's characteristics by controlled compositional alterations in Al-7075 metal matrix composites, the observed variations give useful insights into the link between the content of  $Fe_3O_4$  and RHS and the compression strength that ensues as a consequence of this relationship.

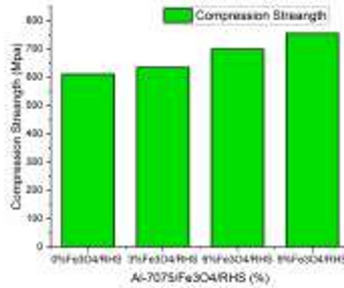


**Fig. 6.** 0 to 9 weight percent composite material with a compression strength of Al7075/ $Fe_3O_4$ /PKSA

### 3.5. An examination of the hardness

Using a Brinell hardness tester, indentation tests were performed on the composite material that the suggested Al matrix alloy was made of. We created specimens of aluminium 7075 alloy with  $Fe_3O_4$ /RHS reinforcement at 3%, 6%, and 9% in accordance with the usual procedures for metallographic analysis. There was a load of 250 kilogrammes of force, a ball with a diameter of 5 millimetres, and a dwell duration of thirty seconds. Recording the indentation load depth readings allowed for the determination of the material's hardness. In order to conduct the indentation test, each specimen was subjected to three iterations of the procedure, and the average data was collected. Hard Iron oxide  $Fe_3O_4$ /RHS is included into the mixture, which results in a progressive rise in the hardness values, which range from 65.7 to 108.75 BHN, as shown in Figure 7. The results of this study emphasise the proportionate increase in hardness that occurs with increasing  $Fe_3O_4$ /RHS particle reinforcement in the Al7075 metal matrix composite.

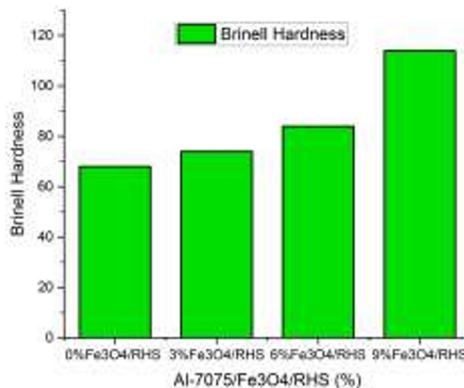


**Fig. 7.** The composite material Al7075/  $Fe_3O_4$ /PKSA has a hardness ranging from 0 to 9 weight percent.

### 3.6. Visual Structure under a Microscope

The Tescan Vega Scanning Electron Microscope was used during the process of conducting a microstructural evaluation of the composites that were manufactured. Cutting test samples with a diameter of 10 to 12 millimetres was done from the castings, and then they were polished with great care. The Al7075/  $\text{Fe}_3\text{O}_4$ /RHS particulate composites are shown in the scanning electron micrographs (SEM) shown in Figure 8 (a-3%  $\text{Fe}_3\text{O}_4$ /RHS, b- 6%  $\text{Fe}_3\text{O}_4$ /RHS, and c- 9%  $\text{Fe}_3\text{O}_4$ /RHS). Particularly noteworthy is the fact that the photos show a uniform distribution of  $\text{Fe}_3\text{O}_4$ /RHS particles with a restricted amount of aggregation, segregation, and porosity. It is essential to note that there is no sign of casting faults like as fractures, slag inclusions, or shrinkages, which substantiates the sound quality of the casting. The microstructural study highlights the effective incorporation of  $\text{Fe}_3\text{O}_4$ /RHS particles into the Al-7075 matrix. It also highlights the uniform distribution of the composite material and the lack of any casting irregularities that might be harmful to its performance.

Figure 8 a-c displays optical micrographs of hybrid composites of varied proportions that are based on Al-7075 and include  $\text{Fe}_3\text{O}_4$  and rice husks ash. These composites are based on Al-7075. Based on the figures, it seems that the distribution of the overall reinforcement appears to be distributed in a way that is distributed evenly. When looking at the Al-7075 alloy, it is able to see the reinforcement that is present not only at the grain boundaries but also inside the grains themselves. Among the matrix alloy and the reinforcements, there is a remarkable metallurgical connection that exists. Furthermore, each and every one of the micrographs demonstrates that there is no damage that can be identified. All of the combinations that were investigated did not exhibit any clustering of reinforcements inside the matrix, and there was a great dispersion of reinforcements as they moved across the matrix. The existence of porosity or cracks in a composite material is a reliable indicator of the substance's overall quality. In the case of the matrix material and the reinforcements, an optical micrograph indicates that there is a strong relationship between the two. In addition to this, data has been produced that serves to indicate the presence of particles in the border region. Gaps and discontinuities are not present inside the reinforced particles; they are completely absent. Expanding the quantity of reinforcing material that is present in the base matrix might result in a reduction in the grain size.

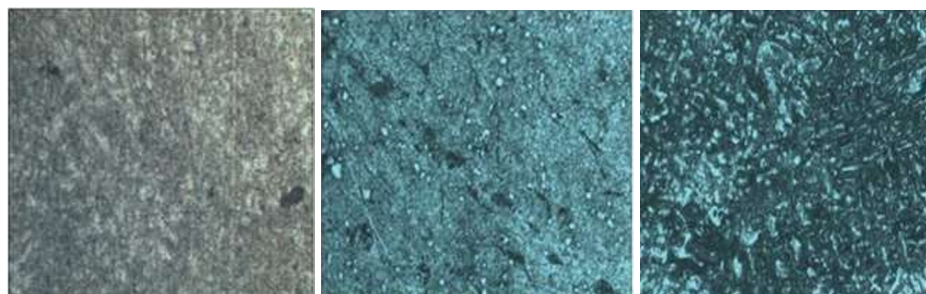


**Fig. 8.** a) 3%RHS/  $\text{Fe}_3\text{O}_4$ .      b) 6%RHS/  $\text{Fe}_3\text{O}_4$ .      c) 9%RHS/  $\text{Fe}_3\text{O}_4$ .

Figures 8 a–c show optical micrographs of the sample. In every instance of hybrid composites, the primary phase of the microstructure was determined to be a-Al, and it was accompanied by nucleation of Mg Zn<sub>2</sub> and Al<sub>2</sub> Cu Mg precipitates. It was discovered that both kinds of precipitates could be found in the intervals between the dendrites, while some Mg Zn<sub>2</sub> precipitates could also be detected in the inside of the dendrites arms. It is

important to keep in mind that the morphology has a significant role in determining whether substances are classified as intermetallics or precipitates.

### 3.7. Surface morphology

For the purpose of identifying material characteristics, scanning electron microscopes (SEMs) that are both highly efficient and versatile are required. The samples are first air-dried using acetone. Figure 9(a-c) shows several microstructures of Al-7075 and a combination of nano-composites. Elongated grains and irregular, acicular particles are seen in Figure 7's structure. When macro-cracks occur in Al-7075, it seems that many globular apatite particles play a role. The matrix retains the microstructure that integrates reinforcing particles because these particles are uniformly dispersed throughout it.

The inclusion of  $\text{Fe}_3\text{O}_4$  and rice husks particles reduces the impact of apatite nucleation, which causes alloy holes and cracks to form (Figure 9b). The uniform dispersion of silica fume particles, as shown in the exterior morphology, proves that the rice husks particles were successfully mixed in. Using a 9% hybrid nano-composite normally results in smaller surface grain sizes for apatite particles. Achieving a consistent distribution of basic elements and distinct subdivisions is the main goal in metallurgy. Figure 9c shows that the refined microstructure, with tiny grains originating from the 9% hybrid nanocomposite, helps to reduce surface fractures and holes. This is because the sector is more resilient and has an equalised morphology.

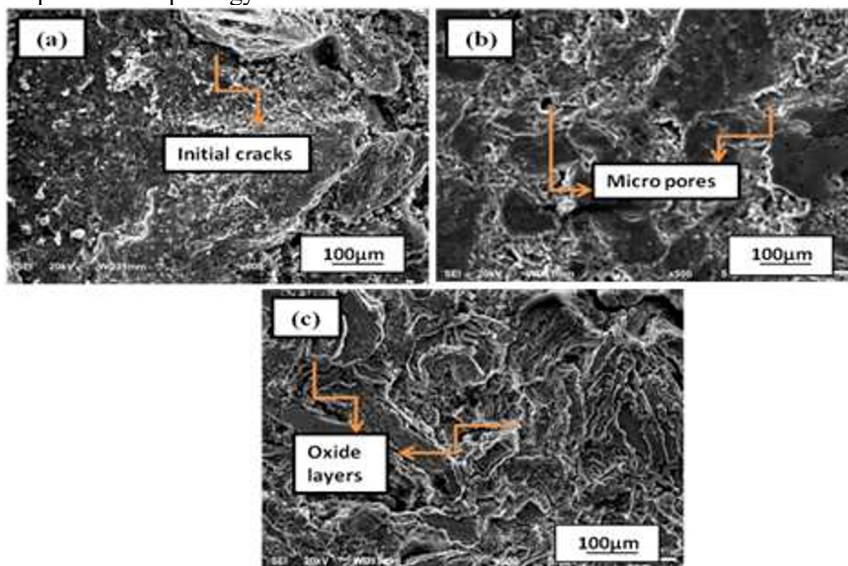


**Fig. 9.** Surface Morphology with [a] Al-7075/3%RHS/  $\text{Fe}_3\text{O}_4$ , [b] Al-7075/6%RHS/  $\text{Fe}_3\text{O}_4$ , [c] Al-7075/9%RHS/  $\text{Fe}_3\text{O}_4$ .

### 3.8. XRD analysis

To examine crystalline materials, scientists use non-destructive X-ray diffraction. Figure 10 (a-c) shows the results of analysing the samples using XRD to determine the amount of  $\text{Fe}_3\text{O}_4$  and rice husks produced at different weight percentages. The important aluminium segments in Figure 10-a of Al-7075 correspond to the direction statistics of JCPDS card 89-4184 [22] and are located at  $2\theta = 23^\circ, 31^\circ, \text{ and } 39^\circ$  orientations. Adding a 3–9 weight

percent mixture composite causes crisp segments and strong signals, suggesting an increase in the Si phase [23], while the matrix's restricted reflection strength gives a qualitative evaluation of the sample crystallinity.

Figure 10-b shows that there are significant XRD reflections when the material becomes very crystalline (with more than 3%  $\text{Fe}_3\text{O}_4$ ). The 6% mixed composite in Figure 10-c shows strong signs with additional peaks at  $2\theta = 20^\circ$ ,  $30^\circ$ , and  $68^\circ$ , which are a result of the increased concentration of rice husks and lower density, which improves the material strength. The dominating C and O peaks clearly show the presence of  $\text{Fe}_3\text{O}_4$  and particles from rice husks. The availability of reinforcements in a 9% mixed composite may reduce the Si and C phases while further enhancing the aluminium segment.

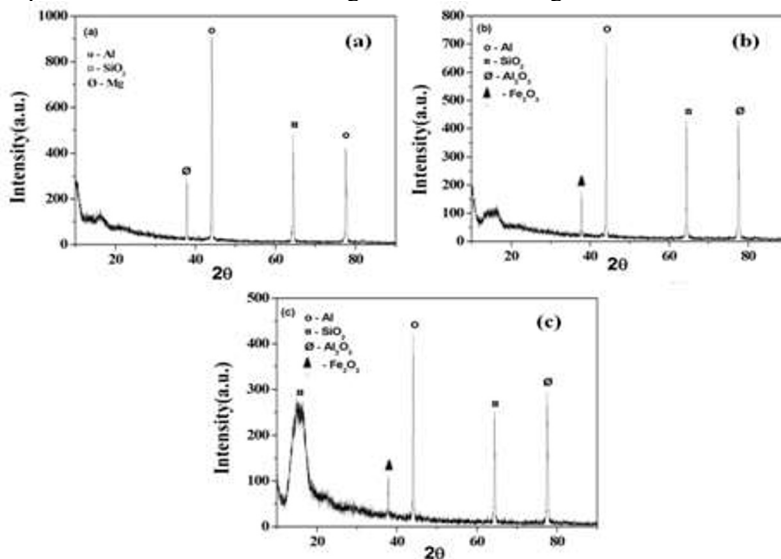


**Fig. 10.** XRD analysis with [a] Al-7075/3%RHS/ $\text{Fe}_3\text{O}_4$ , [b] Al-7075/6%RHS/ $\text{Fe}_3\text{O}_4$ , [c] Al-7075/9%RHS/ $\text{Fe}_3\text{O}_4$ .

#### 4 Findings derived from the current investigation:

The results are arrived at with an average of three values, for the tensile, compression, and Hardness studies.

- ✓ Al-7075 reinforced with 3%, 6%, and 9 %wt  $\text{Fe}_3\text{O}_4$ /RHS Metal Matrix composites fabricated using stir-casting technique with fairly even distribution of particulates in the matrix were effectively produced.
- ✓ The addition of  $\text{Fe}_3\text{O}_4$ /RHS Particulates to the Al-7075 matrix has resulted in enhanced properties in mechanical when related to the Al matrix alone.
- ✓ Corresponding to the result BHN value was dominating the percentage of 9% of  $\text{Fe}_3\text{O}_4$ /RHS. In this process, while the percentage of  $\text{Fe}_3\text{O}_4$ /RHS increases, the higher the value of BHN is noticed.
- ✓ Further, wt. % addition of  $\text{Fe}_3\text{O}_4$ /RHS density and hardness of the composite increases in such a line of attach that retaining the properties of base metal would be the challenging.

- ✓ Corresponding to the surface morphology and XRD Analysis shown the % of reinforcements incremental represents oxide layers.
- ✓ From the SEM images, it can be observed that the distributions of reinforcement are fairly uniform.

Lastly, this study concluded that the stirring process also accountable for the fabrication of composites.

## References

1. F.Q. Tian, N.K. Li, J.Z. Cui, Development process and direction of strengthening and toughening of ultra-high strength aluminum alloy [J], *Light Alloy Process. Technol.* 33 (12) (2005) 1–9.
2. A. Seshappa, B. Anjaneya Prasad Characterization and Investigation of Mechanical Properties of Aluminium Hybrid Nano-composites: Novel Approach of Utilizing Silicon Carbide and Waste Particles to Reduce Cost of Material. *ISSN Silicon*, 1876-990X, 2020, <https://doi.org/10.1007/s12633-020-00748-z>
3. B. Zhou, S. Lu, K.-l. Xu, C. Xu, Z.-Y. Wang, B.-J. Wang, Hot cracking tendency test and simulation of 7075 semi-solid aluminium alloy [J], *Trans. Nonferrous Metals Soc. China* 30 (2) (2020) 318–332.
4. J. Ren, R.C. Wang, Y. Feng, C.Q. Peng, Z.Y. Cai, Microstructure evolution and mechanical properties of an ultrahigh strength Al Zn Mg Cu Zr Sc (7075) alloy processed by modified powder hot extrusion with post aging [J], *Vacuum* 161 (2019) 434–442.
5. J.M. García-Infanta, A.P. Zhilyaev, A. Sharafutdinov, O.A. Ruano, F. Carreño, An evidence of high strain rate superplasticity at intermediate homologous temperatures in an Al Zn Mg Cu alloy processed by high-pressure torsion [J], *J. Alloy. Compd.* 473 (1-2) (2009) 163–166.
6. Z. Horita, T. Fujinami, M. Nemoto, T.G. Langdon, Improvement of mechanical properties for Al alloys using equal-channel angular pressing [J], *J. Mater. Process. Technol.* 117 (3) (2001) 288–292.
7. A. Javdani, A.H. Daeisorkhabi, Microstructural and mechanical behavior of blended powder semisolid formed Al7075/B 4 C composites under different experimental conditions, *Trans. Nonferrous Metals Soc. China* 28 (7) (2018) 1298–1310.
8. J. Hashim, L. Looney, M.S.J. Hashmi, Particle distribution in cast metal matrix composites - part II, *J. Mater. Process. Technol.* 123 (2) (2002) 258–263, [https://doi.org/10.1016/S0924-0136\(02\)00099-7](https://doi.org/10.1016/S0924-0136(02)00099-7).
9. S.K. Pradhan, S. Chatterjee, A.B. Mallick, D. Das, A simple stir casting technique for the preparation of in situ Fe-aluminides reinforced Al-matrix composites, *Perspect. Sci.* 8 (2016) 529–532, <https://doi.org/10.1016/j.pisc.2016.06.011>.
10. E. Bayraktar, D. Katundi, Development of A New Aluminium Matrix Composite Reinforced with Iron Oxide (Fe<sub>3</sub>O<sub>4</sub>) *Journal of Achievements in Materials and Manufacturing Engineering*.
11. J. Liu, Y.-S. Cheng, S.W.N. Chan, D. Sung, Microstructure and mechanical properties of 7075 aluminum alloy during complex this extrusion, *Trans. Nonferrous Metals Soc. China* 30 (12) (2020) 3173–3182, [https://doi.org/10.1016/S1003-6326\(20\)65452-8](https://doi.org/10.1016/S1003-6326(20)65452-8).

12. C.M. Anand Partheeban, M. Rajendran, S.C. Vettivel, S. Suresh, N.S.V. Moorthi, Mechanical behavior and failure analysis using online acoustic emission on nano-graphite reinforced Al6061–10TiB<sub>2</sub> hybrid composite using powder metallurgy, *Mater. Sci. Eng.: A* 632 (2015) 1–13.
13. Trishul M.A, Virupaxayya Hiremath, Shreyas P, Production and Testing of Al- Fe<sub>2</sub>O<sub>3</sub> Particulate Composite. *Journal of Achievements In Materials And Manufacturing Engineering*.
14. [13] Essam R. I. Mahmoud and Mahmoud M. Tash, Characterization of Aluminum-Based-Surface Matrix Composites with Iron and Iron Oxide Fabricated by Friction Stir Processing. *Journal of Achievements in Materials And Manufacturing Engineering*.
15. Emin Bayraktar, Fayza Ayari, Ming Jen Tan, Ayse Tosun-Bayraktar, And DHURATA KATUNDI, Manufacturing Of Aluminum Matrix Composites Reinforced With Iron Oxide (Fe<sub>3</sub>O<sub>4</sub>) Nanoparticles: Microstructural And Mechanical Properties. *Journal Of Achievements In Materials And Manufacturing Engineering*.
16. F. Ayari A, B, D. Katundi B, And E. Bayraktar B, Damage Of Aluminium Matrix Composite Reinforced With Iron Oxide (Fe<sub>3</sub>O<sub>4</sub>): Experimental And Numerical Study. *Journal Of Achievements In Materials And Manufacturing Engineering*.
17. Yi Wang<sup>1,2</sup>, XiaoLan Song<sup>3</sup>, Wei Jiang<sup>1</sup>, Guo-Dong Deng<sup>1</sup>, Xiao-De Guo<sup>1</sup>, Hong-Ying LIU<sup>1</sup>, FengSheng LI<sup>1</sup>, Mechanism For Thermite Reactions Of Aluminum/Iron-Oxide Nanocomposites Based On Residue Analysis. *Journal Of Achievements In Materials And Manufacturing Engineering*.
18. Emin Bayraktar, Fayza Ayari, Ming Jen Tan, Ayse Tosun-Bayraktar, And Dhurata Katundi, Manufacturing Of Aluminium Matrix Composites Reinforced With Iron Oxide (Fe<sub>3</sub>O<sub>4</sub>) Nanoparticles: Microstructure And Mechanical Properties. *Journal Of Achievements In Materials And Manufacturing Engineering*.
19. Palani swamy Shanmugha sundaram<sup>1</sup>, Of Iron Oxide On Tribological Behaviour Of Al- Si Alloy – Iron Oxide Composites – Taguchi Approach. *Journal Of Achievements In Materials And Manufacturing Engineering*.
20. E. Bayraktar, M.-H. Robert, I. Miskioglu, And A. Tosun Bayraktar, Mechanical And Tribological Performance Of Aluminium Matrix, Composite Reinforced With Nano Iron Oxide (Fe<sub>3</sub>O<sub>4</sub>). *Journal Of Achievements In Materials And Manufacturing Engineering*.
21. Kumar GP, Keshavamurthy R, Tambrallimath V, Biswas R, Andhale YS (2018) Mechanical Properties of Al7075-SiC-TiO<sub>2</sub> Hybrid Metal Matrix Composite. In *AdvManuf and Mater Sci* 1:301-307
22. Sambathkumar M, Navaneethkrishnan P, Ponappa KS, Sasikumar KS (2017) Mechanical and corrosion behavior of Al7075 (hybrid) metal matrix composites by two step stir casting process. *Latin Amer J of Solids and Struct* 14:243-55
23. Murali M, Sambathkumar M, Saravanan MS (2014) Micro structural and mechanical properties of AA 7075/TiO<sub>2</sub> in situ composites. *Univer J of Mater Sci* 2:49-53